AAAFM ENERGY

Aromatic Copper Hydride Cages

Jonathan O. Tellechea[1], Carlos Lima[1], Duke Choi[1], Dennis Salazar[1], Marjan Samiei[1],

Angie Keoseyan[1], Ekaterina Vinogradova[2], Fangzhi Yan[3], Daniel Wherritt[3],

Marcos M. Alvarez[1,*], Glen Baghdasarian[1,*], and Robert L. Whetten[2, 4, 5, 6]

[1]Department of Chemistry, Los Angeles City College, Los Angeles, CA 90029
[2]Department of Physics & Astronomy, University of Texas, San Antonio, TX 78249
[3]Department of Chemistry, University of Texas, San Antonio, TX 78249
[4]Department of Applied Physics & Materials Science, Northern Arizona University, Flagstaff, AZ 86011
[5]Department of Chemistry and Biochemistry, Northern Arizona University, Flagstaff, AZ 86011
[6]Center for Materials Interfaces in Research & Applications ¡MIRA!, Northern Arizona University, Flagstaff, AZ 86011

ABSTRACT: Copper clusters are nanoscale materials comprised of a metal core or frame enclosed by a mantle of stabilizing ligands; their exploration offers progress in diverse fields, such as medicine, electronics, and fundamental chemistry as catalysts, reducing agents, corrosion inhibitors, and petroleum sweeteners. When stabilized with dithiocarbamate (DTC) ligands (L), copper clusters show a propensity for reversible hydrogen uptake and a remarkable versatility in size and shape as demonstrated by the facile substitution of the protecting groups and multitude of species attainable. The purpose of this report is to demonstrate the versatility of the Cu-DTC system by the novel use of an aromatic dibenzyl DTC ligand (L') to generate clusters of previously known composition (i.e., $Cu_8HL'_6 PF_6$). As demonstrated herein, the new materials are air stable and amenable to characterization by high-resolution electrospray ionization mass spectrometry, ^1H-nuclear magnetic resonance spectrometry, powder X-ray diffraction, Fourier Transform Infrared Spectroscopy, Ultraviolet-Visible spectroscopy, and Inductively Coupled Plasma Spectrometry. The subject - hydrogen-rich caged cluster materials have potential applications as hydrogen storage sponges to great benefit to material science, energy, and other chemical fields.

KEYWORDS: *Copper, Hydrides, Hydrogen storage, Clusters.*

INTRODUCTION

For decades, hydrogen has been promoted as the transportation fuel of the future because it has the highest energy output per mass and because of its environmentally friendly combustion products: water [1]. The storage of hydrogen fuel in solid matrices (metal hydrides sponges) ameliorates the safety issues associated with its flammability and eliminates the need to cool it and compress it into a liquid. However, solid storage materials are costly, prone to decomposition, corrosion, and overheating upon recharging [2,3]. Copper, the lightest and most affordable of the noble inert metals, has a peculiar affinity toward hydrides that makes it an ideal candidate for a hydrogen storage material.

The study of copper hydride cages is motivated on the one hand by the versatility of copper organic compounds in organic chemistry, and on the other hand, by the added reactivity associated with large surface areas afforded in small dimensions [4]. At the nanoscale, gold particles are excellent oxidation catalysts facilitating the production of aldehydes, ketones, and epoxides from alkenes [5]. At the molecular level, organocuprates or Gilman reagents are classical carbon coupling reagents [6,7]. Copper hydrides (Stryker reagents) find use as reducing agents and copper halide salts catalyze the hydrolysis of allyl halides [7,8]. Recently, the use of a copper catalyst to promote the asymmetric addition of a hydrogen atom and an amine functional group into an inac-

tivated internal alkene has been demonstrated [9]. Copper hydride clusters have been shown to catalyze the hydrogenation of ketones to alcohols [10].

Copper cages and inorganic copper clusters and networks have the potential to function as reagents and catalysts because these entities lie in between the molecular and nano-metallic state and their reactivity is largely unexplored and unpredictable. However, unlike gold and silver, copper nanoparticles pose a major synthesis challenge due to their tendency to oxidize upon exposure to air [11]. Recently, Edwards et al. [12] reported on the synthesis of air-stable copper hydride ion complexes with composition $[Cu_{28}H_{15}L_{12}]PF_6$ where "L" stands for dithiocarbamate (DTC) ligand that stabilizes the central copper core against oxidation. This 28-Cu-atom cluster is capable of storing fifteen (15) hydride (H^-) ions that can be reversibly released as hydrogen (H_2) fuel by controlled changes in temperature, acidity, or ultraviolet light exposure. The reversibility of the hydrogen charging–discharging process, its chemical stability, and its high thermal conductivity render the copper-hydride cluster a promising material for applications in energy and transportation fields. The so-called Chinese puzzle ball is only one of many hydride structures that may be produced with varied copper composition, including Cu_6 [13–16], Cu_7 [17,18], Cu_8 [19–22], Cu_{13} [23], Cu_{14} [24,25], Cu_{18} [26,27], Cu_{20} [25,28,29], Cu_{25} [10,30], Cu_{29} [31], Cu_{32} [32,33], Cu_{53} [34], and Cu_{61} [35]. Recent work in this fertile field, including the use of copper hydride compounds as catalyst, has been summarized by several authors [36–41].

The primary objective of the work described here is to demonstrate the versatility of the copper-DTC cluster system by substituting the diisopropyl ligand (L) in a copper monohydride cluster of known composition and structure [20] ($Cu_8HL'_6\ PF_6$) with an aromatic dibenzyldithiocarbamate ligand (L'). The aromatic clusters are regenerated upon decomposition by the addition of excess borohydride, a desirable property that can lead to the use of these clusters as hydrogen storage materials. The substitution is significant because it imparts the cluster the rigidity, functionality, and stability associated with aromatic groups while suggesting a plethora of other similar substitutions. The new materials are selectively characterized by high-resolution electrospray ionization mass spectrometry (ESIMS), proton nuclear magnetic resonance (^{1}H-NMR) spectrometry, powder X-ray diffraction (pXRD), Fourier Transform Infrared Spectroscopy (FTIR), Ultraviolet-Visible spectroscopy, and Inductively Coupled Plasma Spectrometry (ICP).

RESULTS AND DISCUSSION

The synthesis of copper hydride compounds involves the controlled reaction of copper(I) cation with a reducing agent (lithium borohydride), in the presence of a ligand (protecting agent) in a suitable solvent (Tetrahydrofuran) and under an inert atmosphere (Nitrogen gas blanket). Details are provided in the Supplementary Material. In practice, a multitude of products with varying copper to ligand composition is produced depending on the ligand to copper ratio and other reaction conditions, as testified by the broad list of published structures from the above synthetic approach [20,24,28,30,32,36].

Mass analysis of the product after several months of storage revealed that $Cu_8HL'_6\ PF_6$ is a stable fragment species that dominates the spectra Figure 1, as previously reported.[20]

The inset in Figure 1 represents an isotopic fit of the ESIMS envelope by a singly charged $Cu_8HL_6^+$ fragment, demonstrating that the spectrometer can resolve the complications posed by the existence of two copper isotopes. More significantly, the isotopic fit demonstrates the presence of a hydride in the $Cu_8HL'_6\ PF_6$ cage in accordance with pXRD and 1H-NMR results.

Higher-mass clusters are observable at apparent lower concentrations as doubly and triply charged species (Figure 2) by tuning the parameters of the mass spectrometer.

As is typical of electrospray mass spectra, a number of peaks are apparent in the spectra of Figure 2, most probably associated with multiply charged states of the same species, adducts, and mild fragmentation products of the ionization process. A detailed discussion of each component is beyond the scope of this report that focuses on the abundance and special stability of the Cu_8HL_6 cluster. A major shortfall of the ESIMS technique is that it may be biased to species that are easily ionizable and it may be the case that the overwhelming abundance of the $Cu_8HL'_6^+$ species in Figures 1 and 2 is partly due to this bias in detection. Indeed, the abundance of

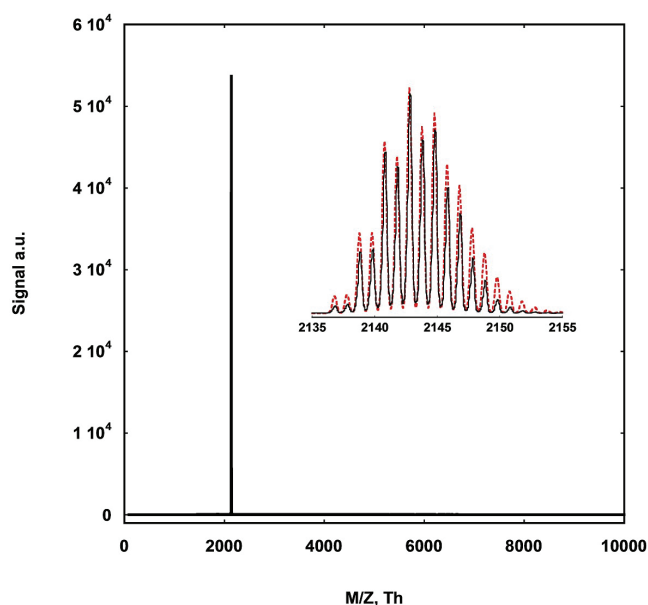**Figure 1. Positive-mode ESIMS analysis of Copper hydride material showing the dominance of $Cu_8HL'_6$ species. Also shown as an inset is the theoretical isotopic distribution fit to $Cu_8C_{90}N_6S_{12}H_{85}$.**

137 the parent $[Cu_{28}H_{15}L_{12}]PF_6$ product in the freshly synthesized
138 material is supported by elemental analysis (Table 1).
139 The experimental Cu/S ratio (1.1) is consistent with the
140 presence of the larger $[Cu_{28}H_{15}L_{12}]PF_6$ (1.2) species in the
141 freshly synthesized product over that of the $Cu_8HL'_6 PF_6$
142 cage (0.67).
143 Although the freshly prepared material is air-stable in
144 solid form, it is susceptible to decomposition when exposed
145 to sunlight and when stored in dichloromethane solution for
146 extended periods of time (days), as judged by its change of
147 color from deep red/orange to yellow (mustard) and olive
148 green. However, the clusters could be regenerated by the
149 addition of excess reducing agent.
150 Powder samples were analyzed for crystallinity in a
151 pXRD instrument using a narrow slit (delta 2 theta = 0.013
152 deg), as summarized in Figure 3, where a geometric correc-
153 tion Sin 2θ has been applied to the intensities.
154 It is clear from the spectrograph that the clusters protected
155 with dibenzyl ligands show long-range order and interplanar
156 spacing of a few nanometers. In addition, it is also apparent
157 that the salient features of the pXRD spectrograph may be
158 attributed to contributions from both the monohydride cage

163 and the empty Cu_8 cage. Indeed, efforts to extract cell param-
164 eters using CMPR—a free access software [42] favored
165 large orthorhombic cells must likely enclosing four cages
166 (a =37.96°A, b = 50.50°A, c = 13.6°A; α—β—δ = 90°). As
167 suspected from the presence of at least two structures, the
168 Figure of Merit of 4.8 is low, given that a value of 10
169 represents a threshold value [43]. The structure of the Cu_8HL_6
170 PF_6 cage reported by others [36] corresponds to a distorted
171 cube (tetracapped tetrahedral, or bicapped octahedral) with
172 a hydride at the center. Upon loss of the endohedral hydride,
173 the cube becomes well defined by eight copper atoms (one
174 per vertex). One dithiocarbamate binds to each of the six
175 faces of the cube. Both structures are sufficiently different to
176 merit future attempts at separation using LC/MS facilities.
177 It is conceivable that the hydride may be also be regener-
178 ated in situ by the intentional addition of a hydrogen source
179 (hydrogen gas or R_3SiH species) rendering the clusters as
180 hydrogenation catalysts and hydrogen storage sponges.
181 According to Edwards's et al. [12], the hydride in the
182 $Cu_8HL_6 PF_6$ species with diisopropyl ligands would appear
183 around 7.05 ppm. Given the fact that the phenyl hydrogens of
184 **L'**, **L'**= $S_2CN(CH_2)_2(C_6H_5)_2$ are in the range of 7.00–7.5 ppm,
185 the hydride in the ^1H NMR spectrum will be hard to detect.
186 However, the integration ratios of **L'** *in that region* are theoret-
187 ically 5:2, while the observed integration ratios (Figure 4) of
188 the Cu_8HL_6 species are slightly higher than the 5:2 ratio which
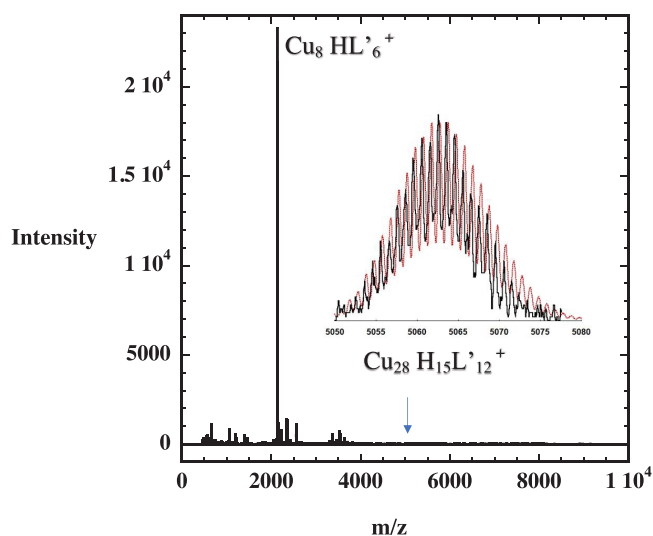189 could suggest that the hydride of $Cu_8HL'_6 PF_6$ is imbedded in
190 the phenyl area.

Figure 2. Positive-mode ESIMS analysis of Copper hydride material showing the presence of the parent species, $Cu_{28}H_{15}L_{12}$ +species. Also shown as an inset is the theoretical isotopic distribution fit to $Cu_{28}C_{180}N_{12}S_{24}H_{183}$.

159 **Table 1. Elemental Analysis of fresh $[Cu_{28}H_{15}L_{12}]PF_6$**
160 **product by ICP compared to expected abundances. Analysis**
161 **performed by Wallace Laboratories, El Segundo, CA.**

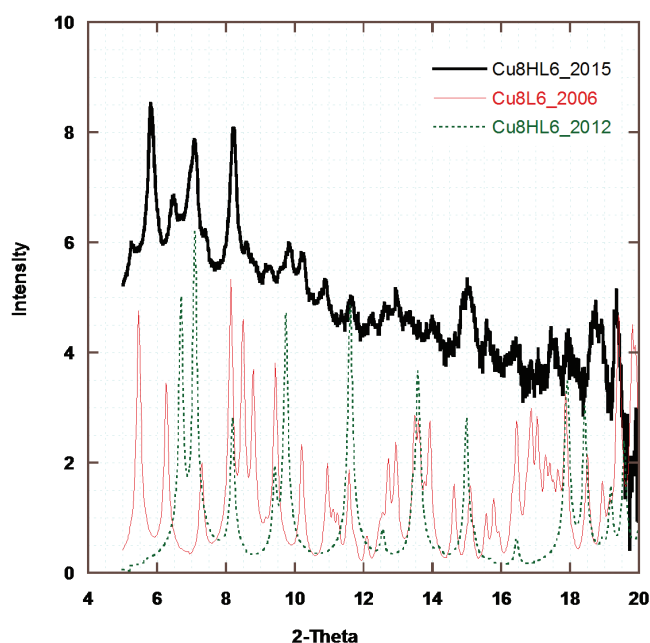| Ratio	ICP	$[Cu_8HL'_6]PF_6$	$[Cu_{28}H_{15}L'_{12}]PF_6$
Cu/S	1.1	0.67	1.2
C/S	10.	7.5	7.5
N/S	0.69	0.50	0.50
P/S	0.054	0.083	0.042

162

Figure 3. pXRD spectrograph of the $Cu_8HL'_6 PF_6$ cage (dark trace) compared to simulated spectra from published single-crystal structures of $Cu_8HL_6^{+17}$ and the empty $Cu_8L_6^{2+}$ with no hydride [22].

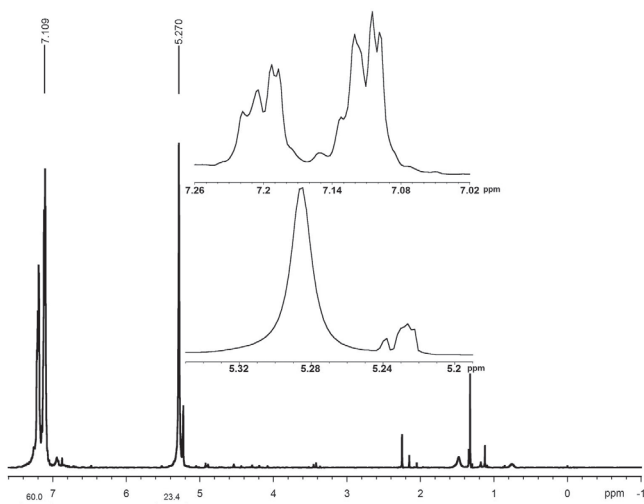**Figure 4.** ^{1}H-NMR (CD$_2$Cl$_2$ 300 MHz) spectrum of **1**.

The phenyl hydrogens and the methylene group were shifted from 7.29 to 7.11 ppm and 5.24 to 5.29 ppm, respectively, which supports the assumption of **L'** being bonded to a copper core as detailed in the Supplementary Material.

A shift in frequencies of key vibrational modes of the ligand was observed by FTIR (Supplementary Material). Most notably, a blue shift in the ν_{C-SS} vibration from 990 to 1,000 cm^{-1} and the existence of a single band in that region is consistent with dibenzyldithiocarbamate anchoring to the copper cage as a bidentate ligand [44].

The optical spectra of the cluster (Figure S6 of the Supplementary Material) is dominated by three bands in the ultraviolet region (255, 295, and 350 nm) typical in dithiocarbamate ligands [45], and an onset of absorption in the visible at 500 nm. There is no evidence for a local surface plasmon band indicative of metal nanoparticles are fine structure of larger molecular clusters [46].

Lower nuclearity clusters such as Cu$_8$HL'$_6$ PF$_6$ have been shown to be fragmentation products of larger clusters [12] and thus are more stable. As such, it is suggested that the added functionality of the substitutions reported here may be exploited to chemically link smaller clusters into a larger, rigid network that may be used as a robust hydrogen storage sponge.

CONCLUSION

The results described above show that cluster hydride materials allow the substitution of different functional groups while retaining well-known stable compositions. These new materials offer ample opportunities for further investigations which may include even larger clusters or cluster networks, of well-known composition and structure, that are copper-rich but in addition to hydrides may incorporate other lighter alloys or intermetallic phases. For example, a copper analog of the famous A$_{145}$X$_{60}$ clusters, wherein normally A = Au or dopant (Ag, Cu, Pd . . .) atoms and X = ligand, would be of great interest. Ongoing research on this subject pursuits the following objectives:

A) Impart coupling functionality to the ligand stabilizing the cluster by attaching a cross-linking carboxylic, amine, organosilane functional group to its terminus.

B) Impart coupling functionality to the cluster: Perform conventional ligand substitution reactions to impart pre-made clusters with the added functionality [29]. Alternative routes to be studied in parallel are to synthesize the cluster using the functionalized ligands and to modify the ligand while attached to the clusters.

C) Synthesize hydrogen sponges by joining the clusters to each other using conventional protein or organosilane conjugation chemistries.

D) Chemically attach/bind the hydrogen sponge onto bulk metallic substrates to enable its use as fuel storage devices and facilitate heat dissipation during recharging of the sponge.

E) Quantify hydrogen-absorption performance and perform H-D exchange experiments to confirm the hydride count.

CONFLICT OF INTEREST

The authors declare that there is no conflict of interest pertaining this publication.

SUPPLEMENTARY MATERIAL

Experimental procedures and characterization data for all new compounds.

REFERENCES

1. Chanchetti LF, Leiva DR, de Faria LI, Ishikawa TT. A scientometric review of research in hydrogen storage materials. Int J Hydrog Energy. 2019. https://doi.org/10.1016/j.ijhydene.2019.06.093

2. Yang J, Sudik A, Wolverton C, Siegel DJ. High capacity hydrogen storage materials: attributes for automotive applications and techniques for materials discovery. Chem Soc Rev. 2010 Feb;39(2):656–75. https://doi.org/10.1039/B802882F

3. Morris L, Hales JJ, Trudeau ML, Georgiev P, Embs JP, Eckert J, et al. A manganese hydride molecular sieve for practical hydrogen storage under ambient conditions. Energy

Environ Sci. 2019;12(5):1580–91. https://doi.org/10.1039/C8EE02499E

4. Gawande MB, Goswami A, Felpin FX, Asefa T, Huang X, Silva R, et al. Cu and Cu-based nanoparticles: synthesis and applications in catalysis. Chem Rev. 2016;116(6):3722–811. https://doi.org/10.1021/acs.chemrev.5b00482

5. Pichugina DA, Kuz'menko NE, Shestakov AF. Ligand-protected gold clusters: the structure, synthesis and applications. Russ Chem Rev. 2015;84(11):1114–44. https://doi.org/10.1070/RCR4493

6. Patureau FW, Gooen LJ. Copper mediated cross coupling reactions. Angew Chem Int Ed. 2014;53:5738–9.

7. Rappoport Z, Marek I. The chemistry of organocopper compounds. Volume 174. Hoboken, NJ: John Wiley & Sons; 2010.

8. Bennett EL, Murphy PJ, Imberti S, Parker SF. Characterization of the hydrides in Stryker's reagent: [HCu{P(C6H5)3}]6. Inorg Chem. 2014;53(6):2963–7. https://doi.org/10.1021/ic402736t

9. Yang Y, Shi SL, Niu D, Liu P, Buchwald SL. ORGANIC CHEMISTRY. Catalytic asymmetric hydroamination of unactivated internal olefins to aliphatic amines. Science. 2015;349(6243):62–6. https://doi.org/10.1126/science.aab3753

10. Sun C, Mammen N, Kaappa S, Yuan P, Deng G, Zhao C, et al. Atomically precise, thiolated copper-hydride nanoclusters as single-site hydrogenation catalysts for ketones in mild conditions. ACS Nano. 2019;13(5):5975–86. https://doi.org/10.1021/acsnano.9b02052

11. Rice KP, Walker EJ Jr, Stoykovich MP, Saunders AE. Solvent-dependent surface plasmon response and oxidation of copper nanocrystals. J Phys Chem C. 2011;115(5):1793–9. https://doi.org/10.1021/jp110483z

12. Edwards AJ, Dhayal RS, Liao P, Liao J, Chiang M, Piltz RO, et al. Chinese puzzle molecule: a 15 hydride, 28 copper atom nanoball. Angew Chem Int Ed Engl. 2014;53(28):7214–8. https://doi.org/10.1002/anie.201403324

13. Churchill MR, Bezman SA, Osborn JA, Wormald J. Synthesis and molecular geometry of hexameric triphenylphosphinocopper (I) hydride and the crystal structure of H6Cu6 (PPh3) 6. HCONMe2 [hexameric triphenylphosphino copper (I) hydride dimethylformamide]. Inorg Chem. 1972;11(8):1818–25. https://doi.org/10.1021/ic50114a015

14. Stevens RC, McLean MR, Bau R, Koetzle TF. Neutron diffraction structure analysis of a hexanuclear copper hydrido complex, H6Cu6 [P (p-tolyl) 3] 6: an unexpected finding. J Am Chem Soc. 1989;111(9):3472–3. https://doi.org/10.1021/ja00191a077

15. Liu CW, Hung CM, Santra BK, Wang JC, Kao HM, Lin Z. Ligand substitution in cubic clusters: surprising isolation of the cocrystallization products of Cu8(μ8-Se)[S2P(OEt)2]6 and Cu6[S2P(OEt)2]6. Inorg Chem. 2003;42(25):8551–6. https://doi.org/10.1021/ic034621f

16. Eberhart MS, Norton JR, Zuzek A, Sattler W, Ruccolo S. Electron transfer from hexameric copper hydrides. J Am Chem Soc. 2013;135(46):17262–5. https://doi.org/10.1021/ja408925m

17. Liao PK, Fang CS, Edwards AJ, Kahlal S, Saillard JY, Liu CW. Hydrido copper clusters supported by dithiocarbamates: oxidative hydride removal and neutron diffraction analysis of [Cu7(H){S2C(aza-15-crown-5)}6] [Cu7 (H){S2C (aza-15-crown-5) 6]. Inorg Chem. 2012;51(12):6577–91. https://doi.org/10.1021/ic300135w

18. Latouche C, Kahlal S, Lin YR, Liao JH, Furet E, Liu CW, et al. Anion encapsulation and geometric changes in hepta- and hexanuclear copper(I) dichalcogeno clusters: a theoretical and experimental investigation. Inorg Chem. 2013;52(22):13253–62. https://doi.org/10.1021/ic402207u

19. Liu CW, Sarkar B, Huang YJ, Liao PK, Wang JC, Saillard JY, et al. Octanuclear copper(I) clusters inscribed in a Se(12) icosahedron: anion-induced modulation of the core size and symmetry. J Am Chem Soc. 2009;131(31):11222–33. https://doi.org/10.1021/ja904089t

20. Wu C, Lee B, Liao P, Fang C, Liu C. Octanuclear Cu (I) dithiophosphates: an efficient catalyst system for NArylation of azoles, amines, and amides. J Chin Chem Soc (Taipei). 2012;59(4):480–4. https://doi.org/10.1002/jccs.201100592

21. Dhayal RS, Liao JH, Hou HN, Ervilita R, Liao PK, Liu CW. Copper(I) diselenocarbamate clusters: synthesis, structures and single-source precursors for Cu and Se composite materials. Dalton Trans. 2015;44(12):5898–908. https://doi.org/10.1039/C4DT03810J

22. Baudron SA, Hosseini MW, Kyritsakas N. Octanuclear Cu (i) cubic complex decorated with six peripheral chelates. New J Chem. 2006;30(7):1083–6. https://doi.org/10.1039/b603733j

23. Chakrahari KK, Liao JH, Kahlal S, Liu YC, Chiang MH, Saillard JY, et al. [Cu13 {S2 CNn Bu2 }6 (acetylide) 4]+ : a two-electron superatom. Angew Chem Int Ed Engl. 2016;55(47):14704–8. https://doi.org/10.1002/anie.201608609

24. Nguyen TA, Goldsmith BR, Zaman HT, Wu G, Peters B, Hayton TW. Synthesis and characterization of a Cu14 hydride cluster supported by neutral donor ligands. Chemistry. 2015;21(14):5341–4. https://doi.org/10.1002/chem.201500422

25. Li YL, Wang J, Luo P, Ma XH, Dong XY, Wang ZY, et al. Cu14 cluster with partial Cu(0) character: difference in electronic structure from isostructural silver analog. Adv Sci (Weinh). 2019;6(18):1900833. https://doi.org/10.1002/advs.201900833

26. Huertos MA, Cano I, Bandeira NA, Benet-Buchholz J, Bo C, van Leeuwen PW. Phosphinothiolates as ligands for polyhydrido copper nanoclusters. Chemistry. 2014;20(49):16121–7. https://doi.org/10.1002/chem.201404763

27. Li J, Ma HZ, Reid GE, Edwards AJ, Hong Y, White JM, et al. Synthesis and X-Ray crystallographic characterisation of frustum-shaped ligated [Cu18 H16 (DPPE)6]2+ and [Cu16 H14 (DPPA)6]2+ nanoclusters and studies on their H2 evolution reactions. Chemistry. 2018;24(9):2070–4. https://doi.org/10.1002/chem.201705448

28. Dhayal RS, Liao JH, Lin YR, Liao PK, Kahlal S, Saillard JY, et al. A nanospheric polyhydrido copper cluster of elongated triangular orthobicupola array: liberation of H2 from solar energy. J Am Chem Soc. 2013;135(12):4704–7. https://doi.org/10.1021/ja401576s

29. Lin PY, Li DY, Ho FH, Liao JH, Barik SK, Liu CW. Unified reciprocity of dithiophosphate by dichalcogenophosph (in) ate ligands on copper hydride nanoclusters via ligand exchange reaction. J Chin Chem Soc (Taipei). 2019;66(9):988–95. https://doi.org/10.1002/jccs.201900086.

30. Nguyen TAD, Jones ZR, Goldsmith BR, Buratto WR, Wu G, Scott SL, et al. A Cu25 nanocluster with partial Cu(0) character. J Am Chem Soc. 2015;137(41):13319–24. https://doi.org/10.1021/jacs.5b07574

31. Nguyen TA, Jones ZR, Leto DF, Wu G, Scott SL, Hayton TW. Ligand-exchange-induced growth of an atomically precise Cu29 nanocluster from a smaller cluster. Chem Mater. 2016;28(22):8385–90. https://doi.org/10.1021/acs.chemmater.6b03879

32. Dhayal RS, Liao J, Kahlal S, Wang X, Liu Y, Chiang M, et al. [Cu32 (H)20 {S2 P(OiPr)2 }12]: The largest number of hydrides recorded in a molecular nanocluster by neutron diffraction. Chemistry. 2015;21(23):8369–74. https://doi.org/10.1002/chem.201501122

33. Dhayal RS, Chen HP, Liao JH, van Zyl WE, Liu CW. Synthesis, structural characterization, and H2 evolution study of a spheroid-shape hydride-rich copper nanocluster. Chemistry Select. 2018;3(13):3603–10. https://doi.org/10.1002/slct.201800765

34. Yuan P, Chen R, Zhang X, Chen F, Yan J, Sun C, et al. Ether-soluble Cu53 nanoclusters as an effective precursor of high-quality CuI films for optoelectronic applications. Angew Chem Int Ed Engl. 2019;58(3):835–9. https://doi.org/10.1002/anie.201812236

35. Ghosh A, Huang RW, Alamer B, Abou-Hamad E, Hedhili MN, Mohammed OF, et al. [Cu61 (StBu) 26S6Cl6H14]+: a core–shell superatom nanocluster with a quasi-J36 Cu19 core and an "18-Crown-6" metal-sulfide-like stabilizing belt. ACS Mater Lett. 2019. Just. Accepted 2019 Jul; https://doi.org/10.1021/acsmaterialslett.9b00122

36. Dhayal RS, van Zyl WE, Liu CW. Polyhydrido copper clusters: synthetic advances, structural diversity, and nanocluster-to-nanoparticle conversion. Acc Chem Res. 2016;49(1):86–95. https://doi.org/10.1021/acs.accounts.5b00375

37. Latouche C, Liu C, Saillard JY. Encapsulating hydrides and main-group anions in d10-metal clusters stabilized by 1, 1-dichalcogeno ligands. J Cluster Sci. 2014;25(1):147–71. https://doi.org/10.1007/s10876-013-0671-3

38. Jordan AJ, Lalic G, Sadighi JP. Coinage metal hydrides: synthesis, characterization, and reactivity. Chem Rev. 2016;116(15):8318–72. https://doi.org/10.1021/acs.chemrev.6b00366

39. Liu X, Astruc D. Atomically precise copper nanoclusters and their applications. Coord Chem Rev. 2018;359:112–26. https://doi.org/10.1016/j.ccr.2018.01.001

40. Dhayal RS, van Zyl WE, Liu CW. Copper hydride clusters in energy storage and conversion. Dalton Trans. 2019;48(11):3531–8. https://doi.org/10.1039/C8DT04639E

41. Paul-Boncour V, Percheron-Guégan A. Synthesis of hydrogen storage materials. Hydrogen storage materials. Berlin, Heidelberg: Springer; 2018. pp. 5–10. https://doi.org/10.1007/978-3-662-54261-3_2

42. Toby BH. CMPRa powder diffraction toolkit. J Appl Cryst. 2005;38(6):1040–1. https://doi.org/10.1107/S0021889805030232

43. Pecharsky VK, Zavalij PY. Fundamentals of powder diffraction and structural characterization of materials. Volume 69. New York, New York: Springer; 2009.

44. Heard PJ. Main group dithiocarbamate complexes. Prog Inorg Chem. 2005;53:1–69.

45. Halls DJ. The properties of dithiocarbamates: a review. Mikrochim Acta. 1969;57(1):62–77. https://doi.org/10.1007/BF01216666

46. Wyrwas RB, Alvarez MM, Khoury JT, Price RC, Schaaff TG, Whetten RL. The colours of nanometric gold. Eur Phys J D. 2007;43(1-3):91–5. https://doi.org/10.1140/epjd/e2007-00117-6

SUPPLEMENTARY INFORMATION

Graphical TOC Entry

METHODS

When producing copper-hydride compounds, the synthesis was performed in tetrahydrofuran using Tetrakis(acetonitrile) copper(I) hexafluorophosphate as the Cu+ source and sodium dibenzyldithiocarbamate as the stabilizing ligand.

Relevant reagents and reaction parameters are summarized in Table S1.

In a typical reproducible synthesis, 3 mmol of Cu(I) where suspended in 10 mL of THF (Slurry A). A second solution was prepared (B) with 1.2 mmol of ligand and 4 mmol of the lithium borohydride reducing agent dissolved in 30 mL of THF. After the system was evacuated and purged, Slurry A was added via cannula injection to Solution B under a constant flow of ultra-high purity nitrogen for one to two hours. As summarized in Figure 1, the reaction products may be purified by evaporation of solvent, washing with methanol, and redissolving in DCM, and precipitation with excess methanol to yield an orange/red solid that could be redissolved in dichloromethane (DCM) and toluene. The exploratory reaction produced clusters with a yield of 30 % (mp. 230-235°C).

Composition was probed via ESI-MS, NMR, and Elemental Analysis. Size and structure were assessed via powder X-Ray Diffraction.

PROTON NUCLEAR MAGNETIC RESONANCE CHARACTERIZATION

The phenyl hydrogens and the methylene group were shifted from 7.29 ppm to 7.11 ppm and 5.24 ppm to 5.29 ppm respectively which can be given credit to **L'** being bonded to a copper core. The theoretical integration ratios are 4:2:4 for the ortho, para, and metal hydrogens, respectively. The para hydrogen is merged into the ortho or meta regions which then yield two regions.[1] Region A has an area of 5 while the area of region B has an area of 6 in respect to the methylene hydrogens. Given that the total area has an integration value of 11 we can extrapolate that a hydride is in region B. From the mass spectrum the abundance of the $[Cu_{28}H_{15}L'_{12}]PF_6$ cluster is small compared to $Cu_8HL'_6$ PF_6 cage. Hence the signals near: 4.20, 1.25, and -0.85 ppm for the $[Cu_{28}H_{15}L'_{12}]PF_6$ hydrides are not noticeable.

MASS SPECTROMETRY ANALYSIS

Mass analysis were performed on a Bruker micrOTOF time-of-flight mass spectrometer with an electrospray ionization source (ESI-MS) using toluene as a solvent. Key operational parameters are summarized below. Isotopic fits to experimental envelops were performed using mMass - open source mass spectrometry tool.[2]

FTIR Characterization

Raw ligand and product were analyzed as compressed powders in a Perkin Elmer Spectrum 100 FTIR spectrometer equipped with an ZnSe ATR accessory. After exhaustive purification, the product shows pronounced IR absorption at 1483 cm^{-1} characteristic of vC-N vibrations with partial double bond character in metal dithiocarbamate complexes (Figure S5).[2] It should be noted that the band is red shifted relative to the starting sodium dibenzyldithiocarbamate

Table S1. Starting reactants for the synthesis of CuH materials.

System	CuHCCC	Molar Quantities
Copper(I) Source	$[Cu(CH_3CN)_4]PF_6$	3 mmol
Ligand	Dibenzyldithiocarbamate	1.2 mmol
Solvent	Tetrahydrofuran	40 mL
Reducing Agent	Lithium borohydride	4 mmol
Work Up	Methanol wash, Crystallization from DCM	

Table S2. Key electrospray ionization mass spectrometer parameters.

Source		Ion Optics		Time of Flight TOF		Processing	
Type	ESI	Capillary Exit	200.0 V	Corrector Fill	40 V	Summation	5000 x
Focus	Not active	Skimmer 1	60.0 V	Pulsar Pull	770 V	Guessed Noise	200
Scan Begin	50 m/z	Hexapole 1	25.0 V	Pulsar Push	770 V	Peak Width	5 pts
Scan End	2000 m/z	Skimmer 2	28.1 V	Reflector	1767 V	Average Noise	10
Ion Polarity	Positive	Hexapole 2	27.0 V	Flight Tube	8600 V	Guessed Average	100
Capillary	4500 V	Hexapole RF	800. V	Corrector Extract	467 V		
End Plate Offset	-500 V	Transfer Time	225.0 µS	TOF Detector	2100 V	Mass Calibration	
Nebulizer	1.0 Bar	Pre-Pulse Storage Time	43 µS			Regression Mode	Linear
Dry Heater	145 oC	Lens1 Storage	50.0 V			C0	201.4898
Dry Gas	5.0 mL/min	Lens 1 Extraction	27.3 V			C1	405780.03
Divert Valve	Source	Lens 2	9.8 V			C2	0
		Lens 3	−30.2 V				
		Lens 4	0.0 V				
		Lens 5	−40.0 V				

(a)   **(b)**   **(c)**
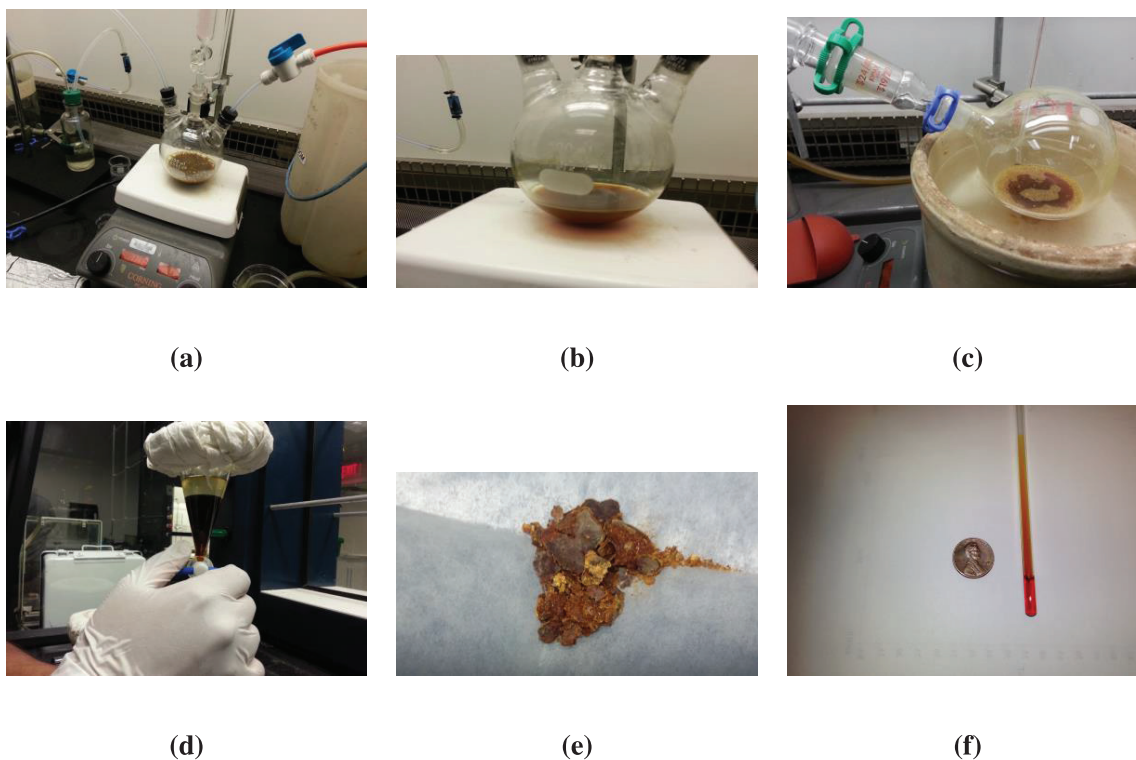
(d)   **(e)**   **(f)**

Figure S1. Synthesis of CuH clusters protected with dibenzyldithiocarbamate ligands.

stock (1493 cm^{-1}). Also noteworthy is the blue shift in νC-SS vibration in the cluster (1000. cm^{-1}) relative to the free ligand (990 cm-1).[4] The blue shift is consistent with a shift from antisymmetric to symmetric vibrational mode associated with a bidentane ligand.[5]

Aromatic νC-H modes are observed at 3030 and 3068 cm are only slightly red The shifting of spectral bands depicted in Figure S5 is significant because it shows that the signal is NOT due to excess ligand unbound to the cluster.

UV-VIS Characterization

The optical spectra of the product (Figure S6) was measured from 240 nm – 800 nm in a Beckman D800 spectrophotometer using Tetrahydrofuran (THF) as
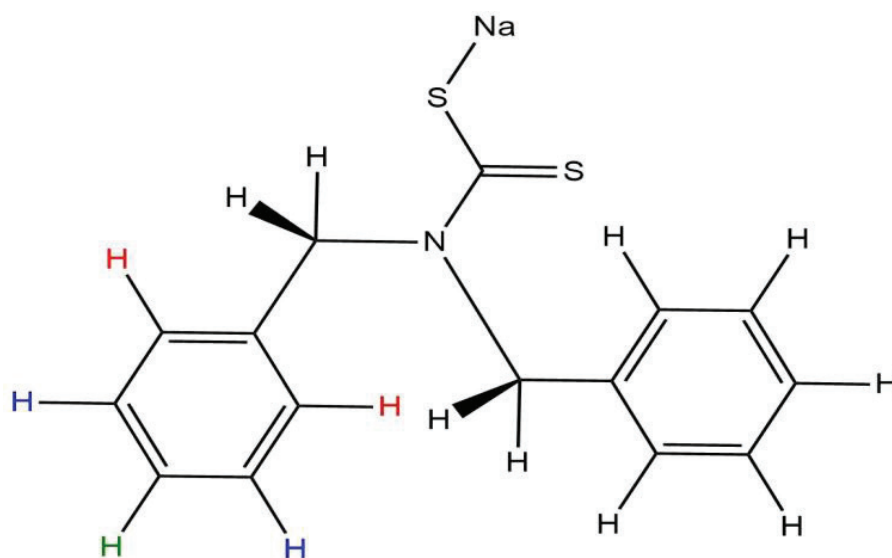
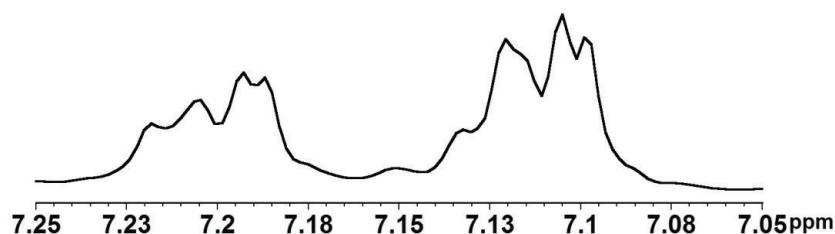**Figure S2. Molecular Structure for L' (sodium N,N-dibenzyldithiocarbamate).**

Figure S3. ¹H NMR (CD2Cl2, 300 MHz) spectrum of Cu8HL'6 PF6 Cage.

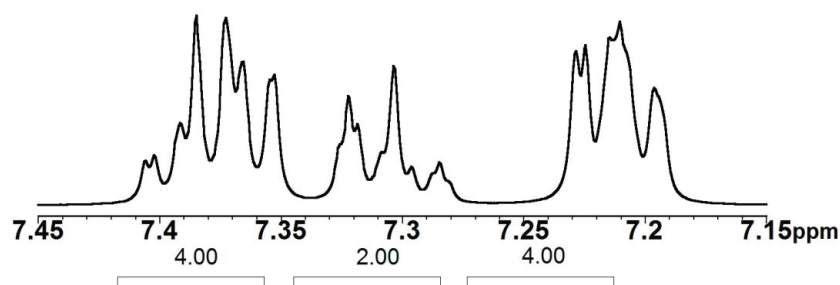**Figure S4. ¹H NMR (CDCl3, 400 MHz) Theoretical spectrum of L'.**

a solvent. The scan started at 240 nm to avoid solvent interference (cut-off frequency of 220 nm). The ultraviolet region of the spectrum is dominated by three bands arising from transitions in the the ligand.[6] The bands at 255nm and 295 nm are due to transitions in the thiocarbonyl group. The salient hump at 350 nm is associated with bonding to nonbonding (n → π*) transitions of electrons in one of the sulfur atoms.[6] The visible region shows a monotonously decaying signal responsible for the amber hue of dilute solutions. An onset of absorption at 500 nm
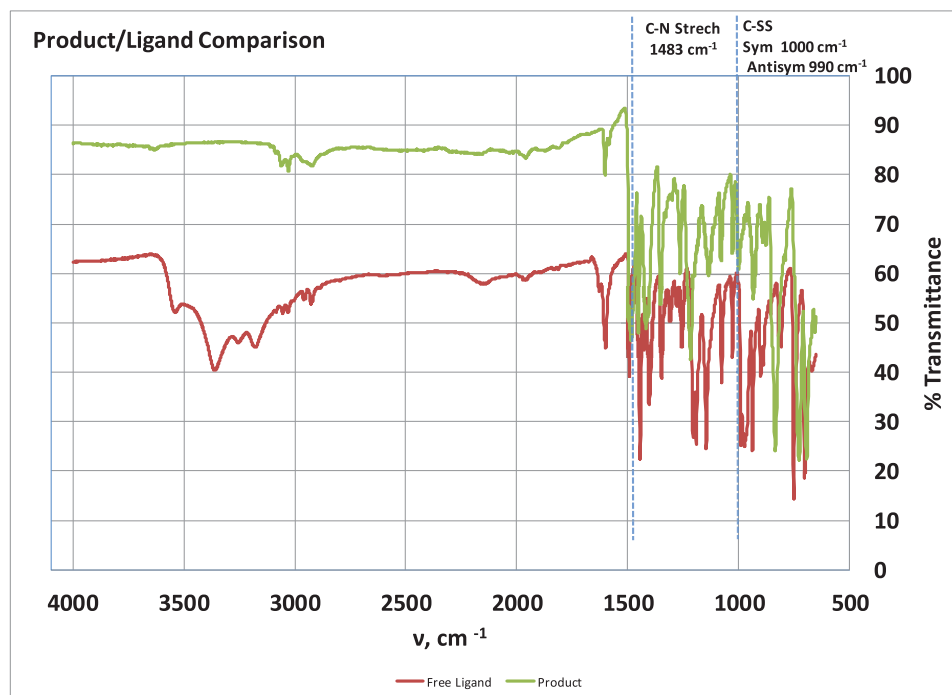
Figure S5. Comparison of FTIR spectral features of product (green trace) to sodium dibenzyldithiocarbamate hydrate (red trace). The spectra of the ligand has been displaced vertically for ease of comparison.
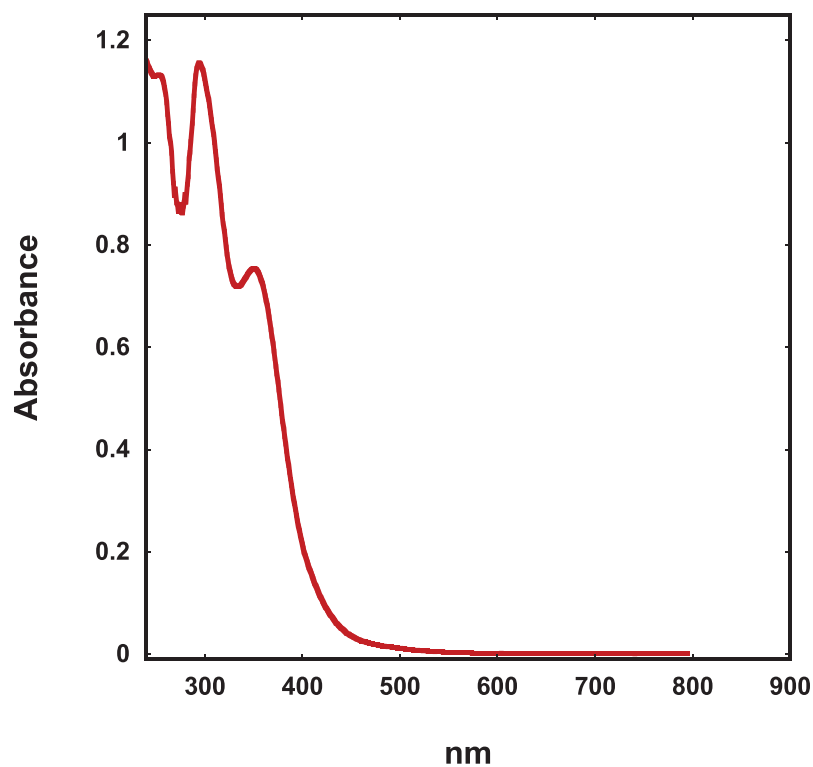

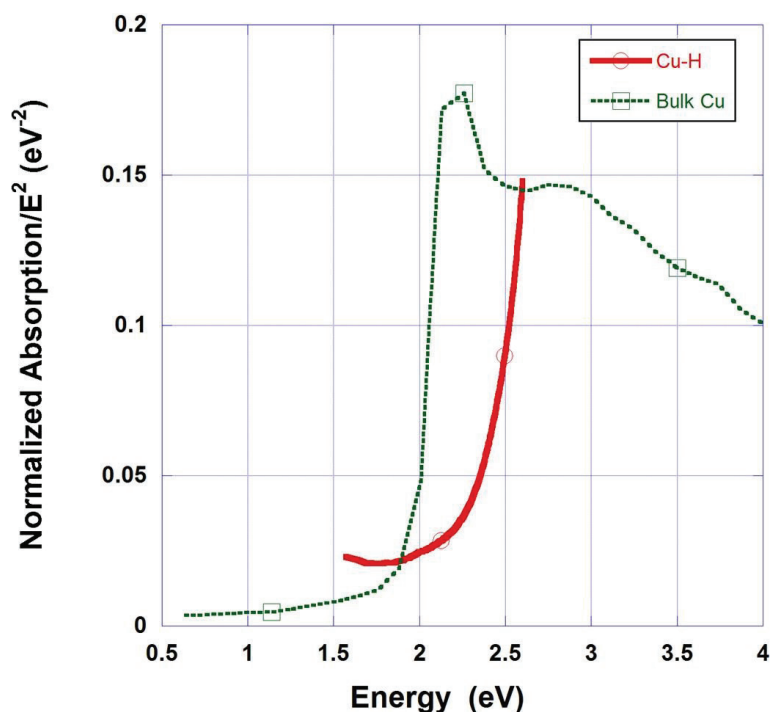**Figure S6. UV-Vis Spectra of Copper Hydride Cluster.**

Figure S7. Optical Absorption of Cu H cluster (red solid trace) compared to spectral features of bulk gold (green dotted trace).

544 (∼ 2.7 eV) is apparent when the absorbance is plotted
545 against photon energy (eV) and the absorbance is scaled
546 as $1/E2$ to facilitate comparison to absorption by bulk
547 gold.[7,8]

548 **REFERENCES**

549 1. Castillo, A. M.; Patiny, L.; Wist, J. Fast and accurate algorithm
550   for the simulation of{NMR} spectra of large spin systems. *J.*
551   *Magn. Reson.* **2011**, 209, 123 – 130.

552 2. Hogarth, G., Transition Metal Dithiocarbamates: 1978–2003.
553   *Progress in inorganic chemistry*, **2005**, *53*, pp.71-561.

554 3. Strohalm, M., Kavan, D., Novak, P., Volny, M. and Havlicek,
555   V., mMass 3: A Cross-Platform Software Environment for
556   Precise Analysis of Mass Spectrometric Data. *Analytical*
557   *chemistry*, **2010**, *82*(11), pp.4648-4651.

558 4. Grigolli, T.M., Cavalheiro, E.T.G., Neto, J.G. and Chierice,
559   G.O., Spectrophotometric Study of Complex Formation
560   Eequilibria of Ni (II) Ion with Benzyl-, Phenyl-and
561   Dibutyldithiocarbamates. *Journal of Solution Chemistry*,
562   **1994**, *23*(7), pp.813-821.

563 5. Gomathi, G., Sathiyaraj, E., Thirumaran, S. and Ciattini, S.,
564   Effect of Functionlization of N, N-dibenzyldithiocarbamate:
565   Synthesis, Spectral and Structural Studies on bis (N-benzyl-
566   N-(4-methoxybenzyl) dithiocarbamato-S, S′) zinc (II) and
567   bis (N-benzyl-N-(4-cholrobenzyl) dithiocarbamato-S, S′)
568   cadmium (II) and their Use for the Preparation of MS (M= Zn,
569   Cd). *Journal of Sulfur Chemistry*, **2016**, *37*(1), pp.23-36.

570 6. Halls, D.J., The Properties of Dithiocarbamates A Review.
571   *Microchimica Acta*, **1969**, *57*(1), pp.62-77.

572 7. Johnson, P.B. and Christy, R.W., 1972. Optical Constants of
573   the Noble Metals. *Physical review B*, *6*(12), p.4370.

574 8. Wyrwas, R. B., M. M. Alvarez, J. T. Khoury, R. C. Price, T. G.
575   Schaaff, and R. L. Whetten. The Colours of Nanometric Gold.
576   *The European Physical Journal D* **2007**, 43, pp. 91-95.